Investigation of the Current Resolution Limits of Advanced Extreme Ultraviolet (EUV) Resists

Patrick P. Naulleau,[1] Clemens Rammeloo,[1] Jason P. Cain,[2] Kim Dean,[3] Paul Denham,[4] Kenneth A. Goldberg,[4]
Brian Hoef,[4] Bruno La Fontaine,[5] Adam R. Pawloski,[5] Carl Larson,[6] and Greg Wallraff [6]

[1] College of Nanoscale Science and Engineering, University at Albany, NY 12203
[2] EECS Department, University of California, Berkeley, CA 94720
[3] SEMATECH, Austin, TX 78741
[4] Center for X-Ray Optics, Lawrence Berkeley National Laboratory, Berkeley, CA 94720
[5] Advanced Micro Devices, Sunnyvale, CA 94088
[6] IBM Almaden Research Center, San Jose, CA 95120

ABSTRACT

The past two years has brought tremendous improvements in the crucial area of resists for extreme ultraviolet (EUV) lithography. Nested and isolated line resolutions approaching 30 nm and 25 nm, respectively, have been demonstrated. These advances have been enabled, in large part, by the high-numerical (0.3) EUV imaging capabilities provided by the Berkeley microfield exposure tool (MET). Here we investigate the resolution limits in several advanced EUV resists using the Berkeley MET. Comparisons to aerial-image performance and the use of resolution-enhancing illumination conditions are used to establish the fact that the observed pattern resolution in the best chemically-amplified resists available today are indeed resist limited. Moreover, contrast transfer function (CTF) techniques are used to directly compare various advanced resists. Strong correlation is observed between relative CTF performance and observed resolution limits.

Keywords: Extreme Ultraviolet, Lithography, Photoresist, Resolution

1. INTRODUCTION

Despite the significant improvements made in extreme ultraviolet (EUV) resists over the past year, resists remain one of the most crucial challenges facing the commercialization of EUV for volume production of nanoelectronics. This is due in large part to the stringent requirement to simultaneously achieve multiple and often opposed characteristics such as high sensitivity, high resolution, and low line edge roughness (LER). For example, one might imagine improving resolution or LER by reducing the speed of the resist, but this is clearly not an option in the realm of commercial-grade EUV resists.

Here we investigate the resolution limits in several advanced EUV resists using the Berkeley microfield exposure tool (MET) 1. Comparisons to aerial-image performance and the use of resolution-enhancing illumination conditions are used to establish the fact that the observed pattern resolution in the best chemically-amplified resists available today are indeed resist limited. We also consider the link between intrinsic bias and resolution and investigate the failure mechanisms in a variety of the most promising EUV resists tested to date. Moreover, contrast transfer function (CTF) techniques are used to directly compare various advanced resists. Strong correlation is observed between relative CTF performance and observed resolution limits.

Emerging Lithographic Technologies X, edited by Michael J. Lercel,
Proc. of SPIE Vol. 6151, 61510Y, (2006) · 0277-786X/06/$15 · doi: 10.1117/12.657005

2. RESOLUTION LIMIT

The measurements presented here are all obtained from the Berkeley MET described in detail elsewhere 2–5. One of the major advantages this tool has over similar MET tools, is the programmable coherence illuminator enabling improved resolution. In principle, the tool with this illuminator supports printing down to a half-pitch of ~12 nm. Another benefit of this tool, is that it has a very well characterized wavefront allowing aerial-image modeling to be used with confidence. This is due, in part, to the at-wavelength interferometry that was used to align the optic on site 6 as well as the quantitative lithographic aberration analysis 2–4 enabled by the programmable illuminator.

We begin by studying the predicted resolution limits of the tool through aerial-image analysis. The analysis is based on the combined interferometric/lithographic wavefront data providing the most accurate picture of the current status of the tool. Figure 1 shows the computed aerial-image contrast as a function of critical dimension (CD) or half-pitch for equal-line-space features. Also shown is a zoom-in on the 45 to 20 nm range further showing the image log slope (ILS). These results assume the standard illumination setting of annular with an inner σ of 0.3 and an outer σ of 0.7. We see the knee in the aerial-image contrast curve to appear at ~25 nm. Refining the analysis through full process window studies, yields the results in Figure 2. Here we plot the double-sided depth of focus (DOF) assuming constraints of 10% exposure latitude (EL), ±10% CD control, greater than 45% contrast, and ILS larger than 20. The DOF results again show a resolution cut-off of ~25 nm.

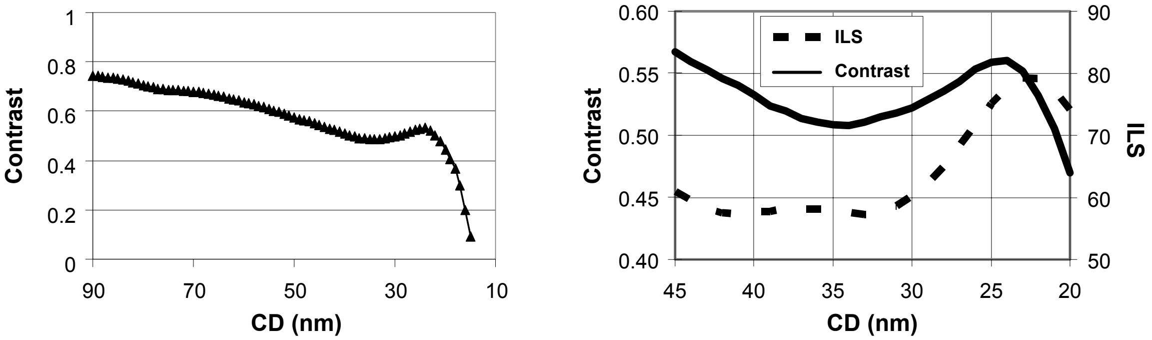

Fig. 1. Computed Aerial-Image Contrast as a Function of CD or Half-Pitch for Equal-Line-Space Features (these results assume the standard illumination setting of annular with an inner σ of 0.3 and an outer σ of 0.7; the analysis is based on the combined interferometric/lithographic wavefront data providing the most accurate picture of the current status of the tool)

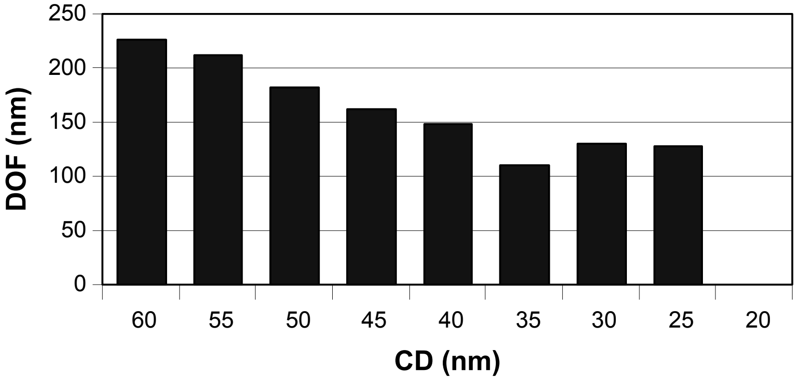

Fig. 2. Full Process Window Studies for the Configuration Described in Figure 1 Plot the Double-Sided DOF Assuming Constraints of 10% EL, ±10% CD Control (greater than 45% contrast) and ILS

In practice, we have not yet observed lithographic-quality printing performance at CDs of 30 nm and smaller 1. We attribute this limitation to the resists themselves. In this section we present data supporting this conclusion and present data from the highest resolving EUV resist tested to date in the Berkeley exposure tool. Referring to Figure 1, we see that for both the ILS and contrast that the values improve as the feature size shrinks from 35 to 25 nm. For comparison, Figure 3 shows a series of equal-line-space images ranging from 45 to 25 nm printed in experimental KRS resist provided by IBM 7. The illumination conditions are as described for the modeling above. Contrary to the results in Figure 1, it is evident that the imaging performance degrades rapidly for sizes below 35 nm, indicating a resist limit as opposed to an aerial-image limit.

Another way to assess a resist limited performance state is to probe printing performance as a function of aerial-image quality. Having a programmable pupil-fill illuminator, the Berkeley system is capable of producing large changes in aerial-image quality at fixed feature sizes (Figure 4). Comparing 35 nm imaging performance, we see that implementing monopole illumination to drive the aerial-image contrast up from ~50% to nearly 70% (y-monopole illumination), we can observe improved imaging performance. Performing the same comparison on 30 nm features, we see virtually no improvement in printing performance (pictures not shown) when going from 50% contrast to nearly 80% contrast (45° monopole).

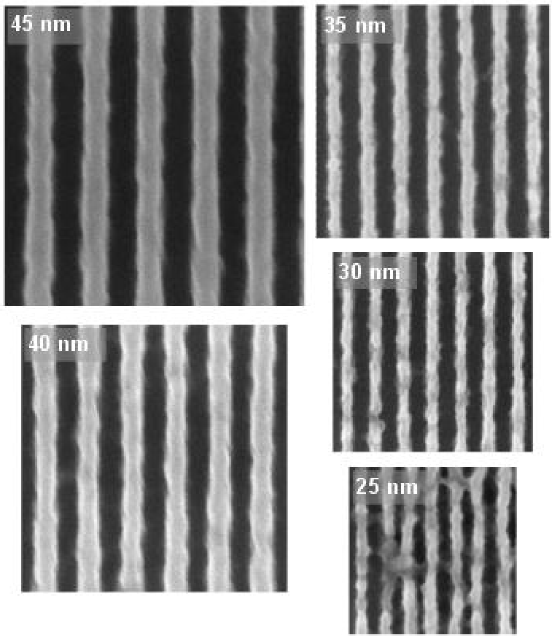

Fig. 3. Equal Line Space Images Ranging from 45 to 25 nm Printed in Experimental *KRS* Resist Provided by IBM (contrary to the results in Figure 5, it is evident that the imaging performance degrades rapidly for sizes below 35 nm, indicating a resist limit as opposed to an aerial-image limit)

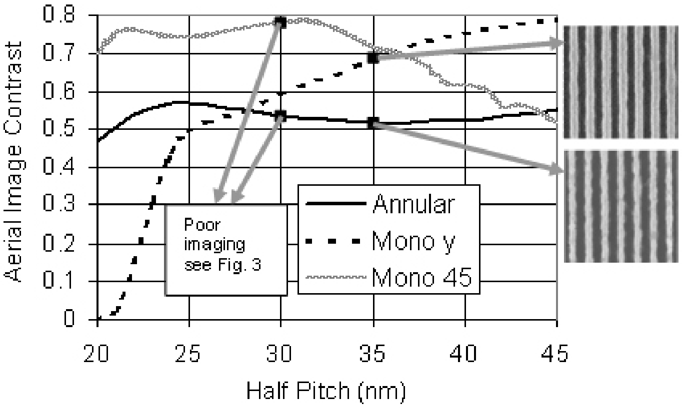

Fig. 4. Computed Aerial-Image Contrast as a Function of CD for Three Different Pupil Fills (comparing 35 nm imaging performance, we see that implementing monopole illumination to drive the aerial-image contrast up from ~50% to nearly 70% [y-monopole illumination], we can observe improved imaging performance; performing the same comparison on 30 nm features, we see virtually no improvement in printing performance [pictures not shown] when going from 50% contrast to nearly 80% contrast [45° monopole])

3. PROCESS WINDOWS AND ISO-FOCAL BIAS

Next we consider iso-focal bias with the goal of seeking a correlation to resolution. Figure 5 shows the aerial-image Bossung curves for 50, 45, and 40-nm features. We see the iso-focal position to be biased up ~5 nm from the coded CD. We also see iso-focal tilt at the 40 nm CD, which we attribute to the spherical error in the wavefront. Figures 6–9 show Bossung curves in four of the best resists tested to date. We see significant differences in iso-focal bias among the resists; however, as evidenced in Figure 10 and summarized in Table 1, there is little correlation between iso-focal bias and resolution.

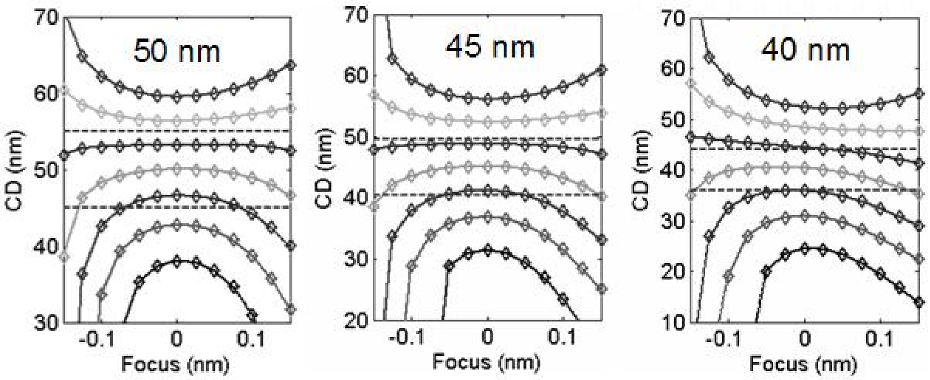

Fig. 5. Aerial-Image Bossung Curves for 50, 45, and 40 nm Features (Bossungs based on 10% dose intervals; we see the iso-focal position to be biased up approximately 5 nm from the coded CD)

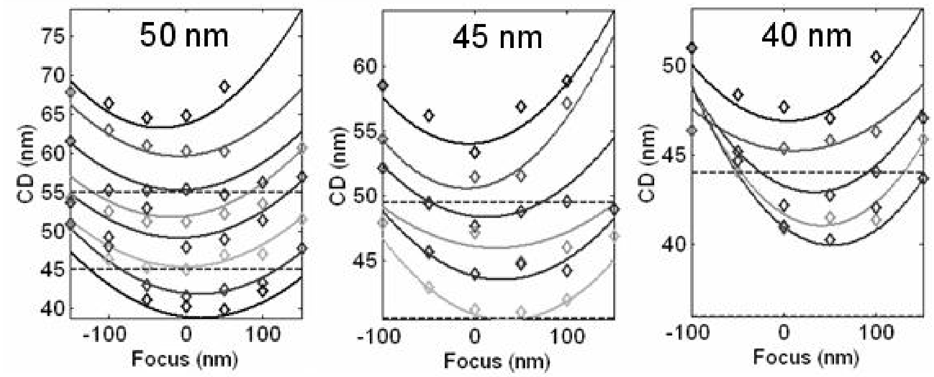

Fig. 6. Bossung Curves for 50, 45, and 40 nm Features in Rohm and Haas MET 1K Resist (Bossungs based on 5% dose intervals)

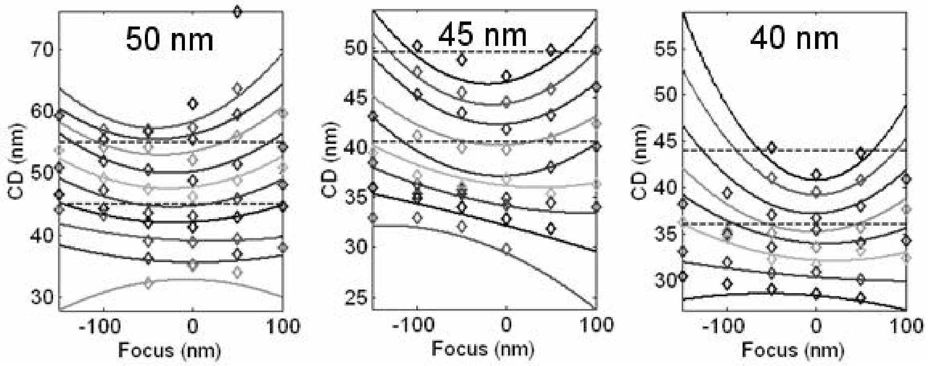

Fig. 7. Bossung Curves for 50, 45, and 40 nm Features in IBM KRS Resist (Bossungs based on 5% dose intervals)

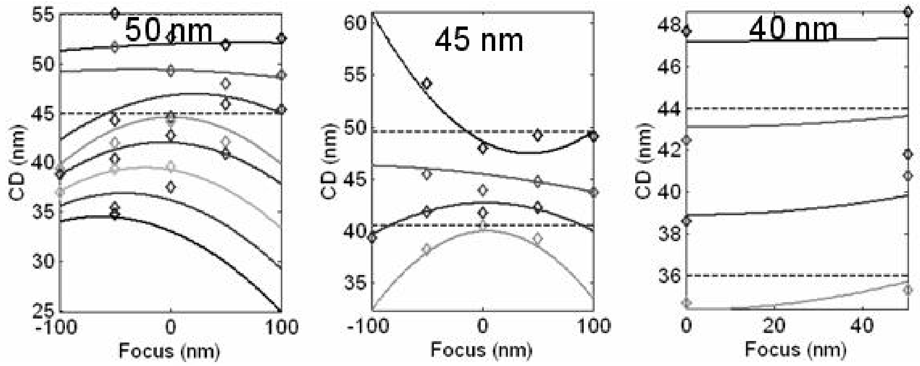

Fig. 8. Bossung Curves for 50, 45, and 40 nm Features in Unnamed Resist A (Bossungs based on 5% dose intervals)

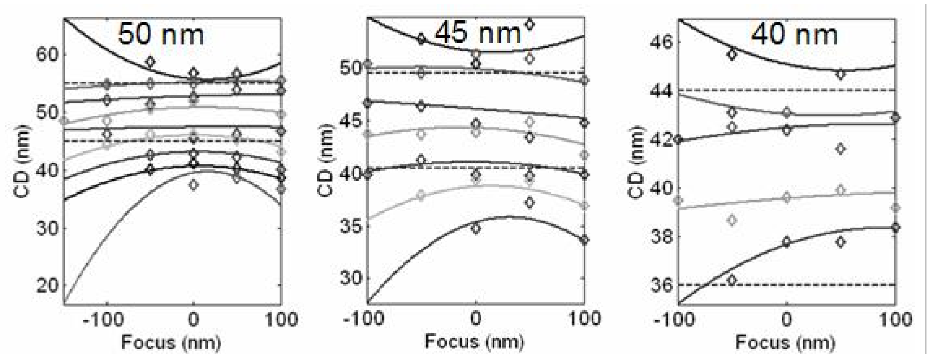

Fig. 9. Bossung Curves for 50, 45, and 40 nm Features in Unnamed Resist C (Bossungs based on 5% dose intervals)

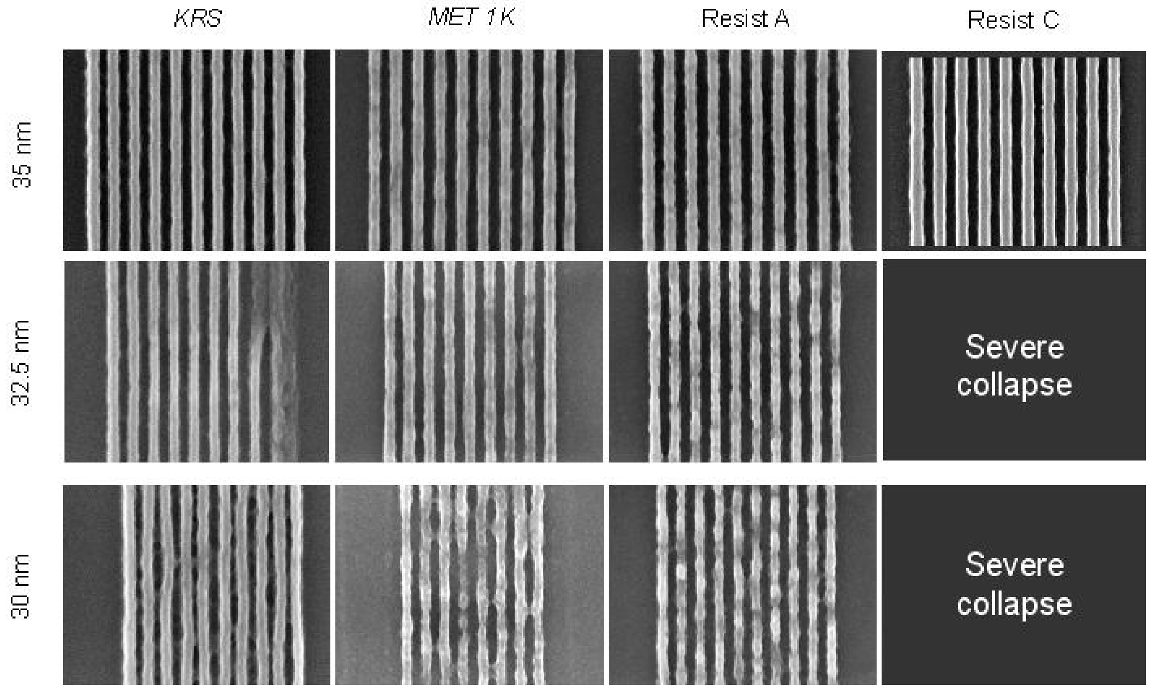

Fig. 10. Resolution Limits for the Four Resists Shown in Figures 6–9 (it is difficult to assess the fundamental resolution limit of Resist C due to its collapse failure mechanism)

Table 1. Summary of Resist Performance Parameters (resolution is defined as the smallest observed well-defined half pitch)

Resist	Speed (mJ/cm^2)	Res. (nm)	LER (nm)	Failure Mechanism	Intrinsic Bias (nm)
Supplier A	11	35	4.5	Top Loss	4
KRS	19	32.5	3.3	Collapse/Top Loss	19
MET 1K	21	35	3.6	Top Loss	> 16
Supplier D	21	45	3.0	Collapse	NA
Supplier C	46	35	2.5	Collapse	4

4. CONTRAST TRANSFER FUNCTION

In light of the difficulties in assessing a subjective criterion such as resolution, it is desirable to find a more rigorously quantitative metric. From the results above, we see that iso-focal bias is not a good predictor of the resolution limit. Next we consider the CTF and its correlation to observed resolution. In practice, the CTF is determined by finding two extreme doses: the first is where the dose is just high enough to cause the lines to begin appearing and the second where the lines are first washed out. These minimum and maximum dose values are then used in the standard contrast definition of (max-min)/(max+min).

Figure 11 shows resulting CTF for the resists characterized above in addition to Rohm and Haas EUV 2D resist (an earlier generation EUV resist with a resolution limit of ~50 nm) as well as the aerial-image CTF.

The plotted results are limited to greater than 35 nm CD to avoid problematic regions of collapse observed in some resists. We find the relative heights of the CTFs to be well correlated to the relative resolution performance of the various resists.

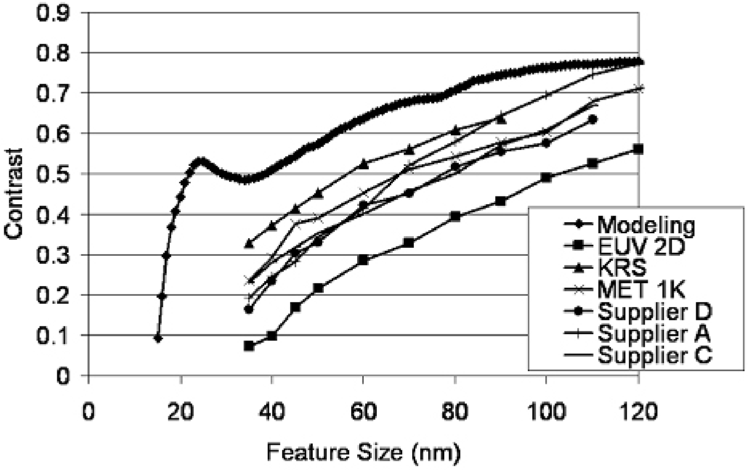

Fig. 11. CTF Measurements for Six Different Resists Compared to the Aerial-Image CTF (we see good correlation between the CTF height and observed resolution limits; results limited to > 35 nm CD to avoid problematic regions of collapse in some resists)

5. SUMMARY

Present imaging performance in the Berkeley MET has been shown to be resist limited. Under the standard annular illumination, the Berkeley system should be capable of lithographic quality 25 nm printing, while resist exposures have performance limited to ~32 nm. A variety of failure mechanisms have been observed among the leading performance resists. Although important as a metric on its own, iso-focal bias was not found as a good predictor of resolution limit. The CTF, on the other hand, shows good correlation to resolution.

ACKNOWLEDGMENTS

The authors are greatly indebted to Paul Denham and Brian Hoef of the Center for X-Ray Optics at Lawrence Berkeley National Laboratory for expert support with the exposure tool as well as the entire CXRO engineering team for bringing the exposure tool to fruition. This research was performed at Lawrence Berkeley National Laboratory and supported by SEMATECH. Lawrence Berkeley National Laboratory is operated under the auspices of the Director, Office of Science, Office of Basic Energy Science, of the US Department of Energy.

REFERENCES

1. P. Naulleau, K. Goldberg, E. Anderson, J. Cain, P. Denham, B. Hoef, K. Jackson, A. Morlens, S. Rekawa, and K. Dean, “EUV Microexposures at the ALS Using the 0.3-NA MET Projection Optics,” Proc. SPIE **5751** 56–63, 2005.
2. P. Naulleau, J. Cain, and K. Goldberg, “Lithographic Characterization of the Spherical Error in an EUV Optic Using a Programmable Pupil Fill Illuminator,” Appl. Opt., *to be published*, 2005.

3. J. Cain, P. Naulleau, and C. Spanos, “Lithographic Measurement of EUV Flare in the 0.3-NA MET Optic,” Proc. SPIE **5751**, 301–311, 2005.
4. P. Naulleau, J. Cain, and K. Goldberg, “Lithographic Characterization of the Field Dependent Astigmatism and Alignment Stability of a 0.3 Numerical Aperture EUV Microfield Optic,” *J. Vac. Sci. & Technol. B*, *to be published*, 2005.
5. P. Naulleau, K. Goldberg, E. Anderson, K. Bradley, R. Delano, P. Denham, B. Gunion, B. Harteneck, B. Hoef, H. Huang, K. Jackson, G. Jones, D. Kemp, A. Liddle, R. Oort, A. Rawlins, S. Rekawa, F. Salmassi, R. Tackaberry, C. Chung, L. Hale, D. Phillion, G. Sommargren, and J. Taylor, “Status of EUV Microexposure Capabilities at the ALS Using the 0.3-NA MET Optic,” Proc. SPIE **5374**, 881–891, 2004.
6. K. Goldberg, P. Naulleau, P. Denham, S. Rekawa, K. Jackson, E. Anderson, and J. Liddle, “EUV Interferometric Testing and Alignment of the 0.3-NA MET Optic,” Proc. SPIE **5374**, 64–73, 2004.
7. Resist provided by G. Wallraff and C. Larson, IBM Almaden Research Ctr., San Jose, CA.